Title	Electric-field driven source of photocarriers for tunable electron spin polarization in InGaAs quantum dots
Author(s)	Kise, Hiroto; Hiura, Satoshi; Park, Soyoung; Takayama, Junichi; Sueoka, Kazuhisa; Murayama, Akihiro
Citation	Applied physics letters, 122(23), 232405 https://doi.org/10.1063/5.0151467
Issue Date	2023-06-05
Doc URL	http://hdl.handle.net/2115/92574
Rights	This article may be downloaded for personal use only. Any other use requires prior permission of the author and AIP Publishing. This article appeared in Appl. Phys. Lett. 122, 232405 (2023) and may be found at https://doi.org/10.1063/5.0151467.
Type	article
File Information	232405_1_5.0151467.pdf

Applied Physics Letters

RESEARCH ARTICLE | JUNE 08 2023

Electric-field driven source of photocarriers for tunable electron spin polarization in InGaAs quantum dots

Hiroto Kise ; Satoshi Hiura ; Soyoung Park ; Junichi Takayama ; Kazuhisa Sueoka;
Akihiro Murayama

Appl. Phys. Lett. 122, 232405 (2023)
https://doi.org/10.1063/5.0151467

AIP Publishing

Applied Physics Letters ARTICLE pubs.aip.org/aip/apl

Electric-field driven source of photocarriers for tunable electron spin polarization in InGaAs quantum dots

Cite as: Appl. Phys. Lett. **122**, 232405 (2023); doi: 10.1063/5.0151467
Submitted: 22 March 2023 · Accepted: 20 May 2023 ·
Published Online: 8 June 2023

Hiroto Kise, Satoshi Hiura,[a)] Soyoung Park, Junichi Takayama, Kazuhisa Sueoka, and Akihiro Murayama

AFFILIATIONS

Faculty of Information Science and Technology, Hokkaido University Kita 14, Nishi 9, Kita-ku, Sapporo 060-0814, Japan

[a)]Author to whom correspondence should be addressed: hiura@ist.hokudai.ac.jp

ABSTRACT

Electric-field control of spin polarization of electrons during injection into InGaAs quantum dots (QDs) was studied via circularly polarized time-resolved photoluminescence. Electric-field modulation of optical spin polarization in QDs will play a key role in future progress of semiconductor opto-spintronics. The tuning of band potentials by applying external electric fields can not only affect spin-injection efficiencies but also switch dominant spin-injection layers. In this study, we developed a QD-based electric-field-effect optical spin device with two different spin-injection layers, which consisted of a GaAs and GaAs/$Al_{0.15}Ga_{0.85}As$ superlattice (SL) barriers. The bias-voltage modulation of the optical spin polarization in QDs was demonstrated by changing the spin polarization degree of electrons injected from these barriers into the QD via the electric-field switching of the spin-injection layers. This was achieved by exploiting the difference in spin relaxation properties between bulk GaAs and the SL. This proposed structure, which comprised of one luminescent layer and two spin-injection layers, is highly scalable because the modulation range of optical spin polarization can be enhanced by changing the combination of spin-injection layers, as well as the material used and its layer thickness.

Spintronics has attracted considerable attention owing to the significant reduction in the electric-power consumption of electronic devices and the performance enhancement of conventional semiconductor-based devices by utilizing the spin polarization of electrons as an information carrier.[1–6] In particular, the development of opto-spintronics devices based on III–V compound semiconductors,[7–13] which can directly convert spin information between electron spin and circularly polarized light via the optical-transition selection rule,[14] is crucial for realizing spin-based photoelectric information systems. III–V semiconductor quantum dots (QDs) are promising materials for the active layer of spin-functional optical devices because of their excellent optical and spin properties.[15–17] QDs exhibit a high luminescence efficiency due to the strong overlap of electron and hole wavefunctions in a small space.[18] In addition, carrier spin relaxation can be significantly suppressed in QDs by the motional freezing of carriers, originating from three-dimensional quantum confinements.[19] Therefore, photoelectric spin conversion using QDs can be a key technology to support the progress of semiconductor opto-spintronics.

For III–V semiconductor-based opto-spintronics, electric-field control of electron spin polarization, corresponding to the circular polarization property of light emission, is essential. Electric-field-dependent photoluminescence (PL) circular polarization has recently been observed in $In_{0.5}Ga_{0.5}As$ QDs tunnel-coupled with an $In_{0.1}Ga_{0.9}As$ quantum well (QW).[20–22] This was achieved via electric-field control of the spin-flip scattering rate within QDs via precise control of the tunnel injection efficiency of electrons and holes, depending on the coupled potential modification. Because the spin-injection layer, where electrons are injected into the QDs, in this structure mainly consists of a QW, the spin polarization degree of electrons, during injection into the QDs, does not depend on the electric-field.[22] This implies that the electric-field-induced change in the electron spin polarization occurs only after injection into the QDs, and this can limit the modulation range of optical spin polarization in QDs.

In this study, we developed a QD-based electric-field-effect optical spin device with two different spin-injection layers, which consisted of a GaAs and GaAs/$Al_{0.15}Ga_{0.85}As$ superlattice (SL) barriers. The spin polarization of electrons can be easily lost in the bulk GaAs,[23,24] whereas it can be conserved in the SL because of the wavefunction overlap of adjacent QWs. The quantum tunneling transport of spin-polarized electrons from the GaAs/$Al_{0.15}Ga_{0.85}As$ SL barrier to

$In_{0.5}Ga_{0.5}As$ QDs has recently been demonstrated, where the electron spin polarization can be fully retained during injection into the QDs.[25,26] Here, we demonstrated the bias-voltage modulation of the optical spin polarization in QDs by changing the spin polarization degree of the electrons injected into the QDs via electric-field switching of the spin-injection layers.

Figure 1(a) shows a schematic of the electric-field-effect optical spin device used in this study. A single layer of 6-ML-thick $In_{0.5}Ga_{0.5}As$ QDs was grown on a p-doped GaAs(100) substrate via molecular beam epitaxy. The QDs were sandwiched between a GaAs and SL barriers of thickness 50 and 165 nm, respectively. The SL consisted of 11 repeats of a GaAs QW and $Al_{0.15}Ga_{0.85}As$ barrier with a thickness of 10 and 5 nm, respectively. Details regarding the sample growth and structural characterization of QDs are presented in the supplementary material (Fig. S1). A Fe/Au electrode, with an optical window for optical excitations and PL observations, was deposited on the semiconductor surface for the application of external electric fields along the growth direction. The GaAs cap layer was heavily p-doped (doping concentration of $6 \times 10^{17}\,cm^{-3}$) to supply sufficient holes to the QDs. This heavy p-doping led to a hole-rich condition in the QDs regardless of the bias voltage; thus, the QD PL intensity and its circular polarization property depended mainly on the electron spin injected into the QDs.

Circularly polarized PL and its time-resolved experiments were conducted at 4 K under σ^+-polarized excitation with the application of a bias voltage. The bias voltage was changed from -2 to $+2$ V. The excitation energy was set to 1.51 and 1.55 eV for optically generating electron spins in the GaAs and SL barriers, respectively, as shown in Fig. 1(b). The electron spin polarization generated in these barriers is expected to be 50%, according to the optical-transition selection rule considering a valence-band mixing.[25,26] Here, the circular polarization degree (CPD) of the QD PL is defined as $(I_{\sigma+} - I_{\sigma-})/(I_{\sigma+} + I_{\sigma-})$, where $I_{\sigma\pm}$ represents the $\sigma^{\pm}$-polarized PL intensity. The CPD value reflects the electron spin polarization in QD states.[22] Details regarding the optical characterization are presented in the supplementary material.

Figures 1(b) and 1(c) show the one-dimensional calculated band profiles in the region from the GaAs barrier to the SL barrier and carrier wavefunctions in the SL barrier at bias voltages of $+1.0$ and -1.0 V, respectively. These calculations were performed using the nextnano software.[27] At $+1.0$ V, the conduction-band potential of the SL barrier tilts toward the QD side, while that of the GaAs barrier exhibits the opposite behavior. Under this condition, most of the electron spins injected into the QDs should originate from the SL barrier. This calculation result suggests the possibility of spin-conserved electron transport to the QDs via phonon-assisted tunneling. In contrast, holes are mainly injected from the GaAs barrier, as the valence band tilted toward the QD side. At -1.0 V, the conduction-band potential of the GaAs barrier tilts toward the QD side. In this case, a significant electron injection should occur from the GaAs barrier into the QDs. These results suggest that the dominant spin-injection layers can be switched by changing the bias voltage.

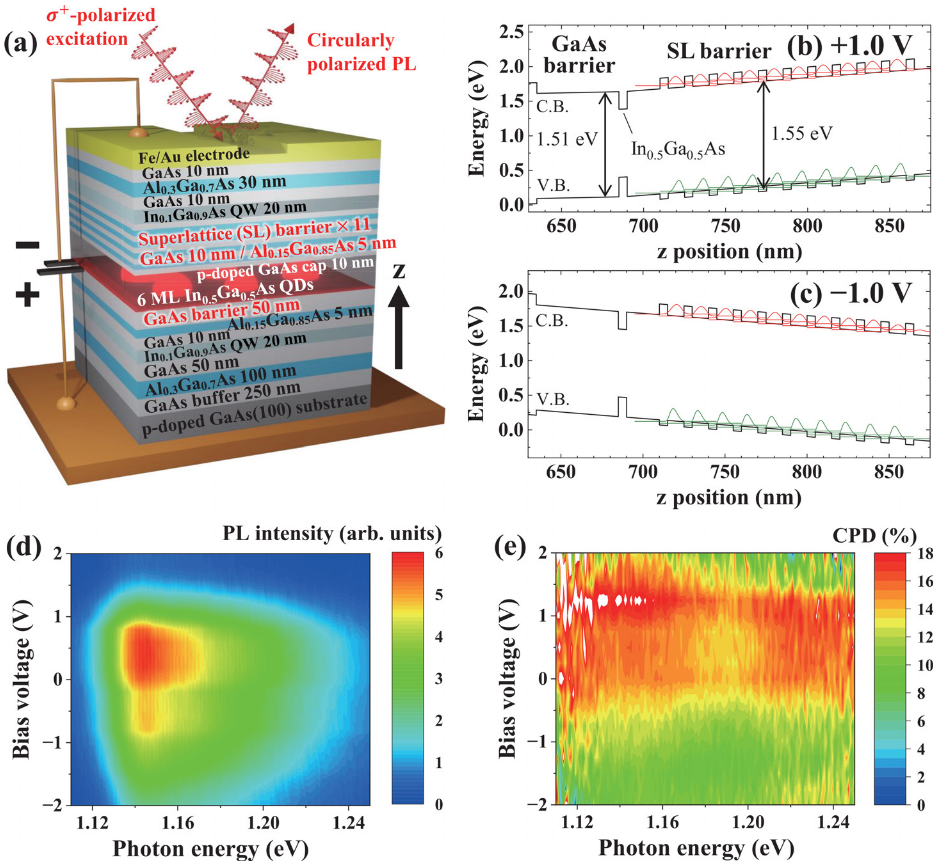

FIG. 1. (a) Schematic of the electric-field-effect optical spin device used in this study. One-dimensional calculations of band profiles with electron and hole wavefunctions in the GaAs/$Al_{0.15}Ga_{0.85}As$ SL barrier at bias voltages of (b) $+1.0$ and (c) -1.0 V. Contour maps indicating the bias-voltage dependence of the (d) PL intensity and (e) CPD with respect to the photon energy at 4 K under σ^+-polarized excitation of the SL barrier with an excitation power of 65 μW.

Figures 1(d) and 1(e) show contour plots of the QD PL intensity and CPD value, respectively, measured under excitation of the SL barrier with an excitation power and energy of 65 μW and 1.55 eV, respectively. Strong PL emissions appear over a wide energy range at the bias voltages ranging from 0 to +1.0 V. According to the calculation results presented above, the higher PL intensity at positive bias voltages implies significant electron injections from the SL barrier into the QDs, and this reflects the larger total thickness of the optically excited GaAs layers. Higher CPD values are also observed at positive bias voltages. The CPD increased from ~10% at −1.0 V to ~18% at +1.0 V around 1.15 eV, corresponding to the QD ground state (GS). To confirm that the bias-voltage-dependent CPD properties are affected by the spin polarization of electrons injected from the barriers, it is necessary to investigate the CPD properties of the QD excited states, which depend on the degree of spin relaxation in the barrier.[25]

Next, we investigated the CPD properties of the QD second excited state (ES2). Figures 2(a) and 2(b) show the circularly polarized PL spectra and their corresponding CPDs at +1.0 and −1.0 V, respectively, measured with an excitation power of 510 μW, under the excitation of the SL barrier. Here, a high excitation power was used to obtain sufficient PL emission from QD ES2; a small shoulder at 1.27 eV is observed, in addition to the two peaks at 1.15 and 1.20 eV. The two lower-energy peaks correspond to the PL emission from the QD GS and first excited state (ES1), and the small shoulder originates from the QD ES2 (Fig. S2). At both bias voltages, the CPD values for the QD GS were far lower than those for the QD ES2. The reduced CPD values were due to the state filling effect at high excitation powers.[28,29] However, a higher CPD of ~30% was observed at +1.0 V, in comparison with ~20% at −1.0 V, at an energy of 1.27 eV. This result is consistent with the dependence of the CPD on the bias-voltage observed in the QD GS at a lower excitation power [Fig. 1(e)]. This confirms the switching of the spin-injection layers between +1.0 and −1.0 V.

Figures 2(c) and 2(d) show the normalized PL intensity and CPD of QD ES2, respectively, with respect to the bias voltage under excitation of the SL and GaAs barriers. Here, the normalized PL intensity was obtained via analysis of the sum of the σ^+- and σ^--polarized PL intensities, and the QD ES2 was defined as the energy range of 1.25–1.29 eV. The bias-voltage dependences of the PL intensity and CPD were affected by the excitation layers. For the excitation of the SL barrier, the PL intensity was higher at a positive bias voltage than at a negative bias voltage. This is attributed to the fact that the total thickness of the optically excited GaAs layer was larger for the SL barrier than for the GaAs barrier, as described above. However, the opposite trend is observed for the excitation of the GaAs barrier. Under this condition, no electrons were generated in the SL barrier, leading to a significant reduction in the PL intensity at positive bias voltages. This result indicates that, under excitation of the SL barrier, electrons were efficiently injected from the SL barrier into the QDs at positive bias voltages. The bias-voltage dependences of the CPD properties further support this conclusion. There CPD values did not exhibit significant changes between −1.0 and +1.0 V for the excitation of the GaAs barrier, whereas the CPD increased from 20% at −1.0 V to 31% at +1.0 V for the excitation of the SL barrier. This indicates that as the positive bias voltage increased, the electron spin injection from the SL barrier into the QDs can be enhanced. Therefore, these results suggest that the gradual increase in the CPD between −1.0 and +1.0 V was due to the increasing spin polarization degree of the injected electrons.

Next, time-resolved measurements of the CPD were conducted to examine the spin polarization properties of electrons during injection into the QDs. Figures 3(a) and 3(b) show the circularly polarized PL spectra and corresponding CPDs at +1.0 and −1.0 V, respectively, measured with an excitation power of 1 mW under excitation of the SL barrier. A far slower PL rise at +1.0 V than at −1.0 V was clearly observed (see the red arrows). We performed a rate-equation

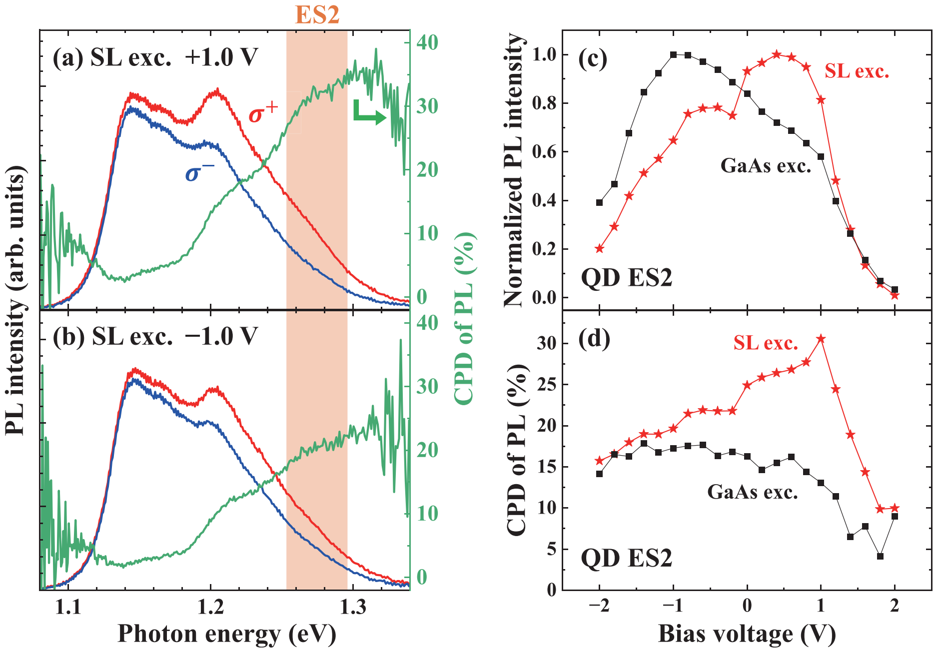

FIG. 2. Circularly polarized PL spectra and corresponding CPDs at 4 K under σ^+-polarized excitation of the SL barrier with an excitation power of 510 μW at bias voltages of (a) +1.0 and (b) −1.0 V. The orange area represents the analyzed energy range of QD ES2. (c) Normalized PL intensity and (d) PL CPD of QD ES2 with respect to the bias voltage under σ^+-polarized excitation of the SL and GaAs barriers.

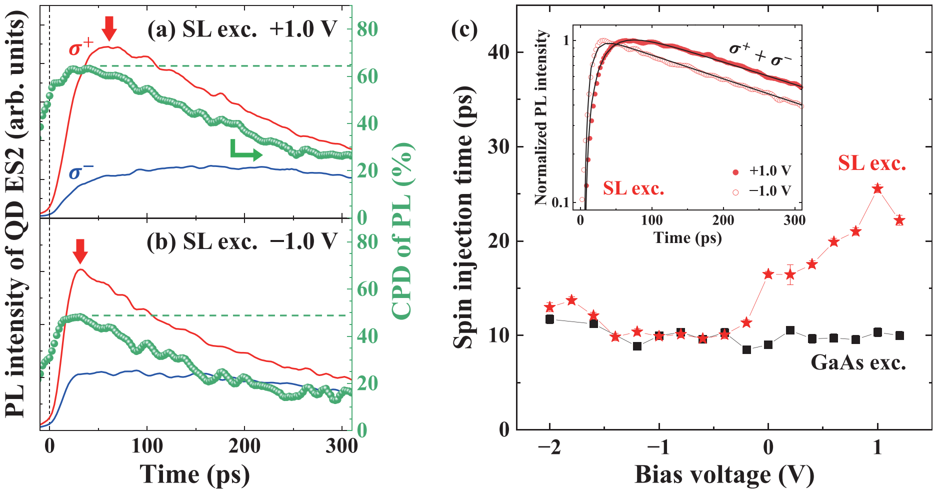

FIG. 3. Circularly polarized PL time profiles and the corresponding CPDs of the QD ES2 at 4 K under σ^+-polarized excitation of the SL barrier with bias voltages of (a) +1.0 and (b) −1.0 V. The red arrows indicate the time positions at which the PL intensity was maximum. (c) Bias-voltage dependence of the spin injection time under σ^+-polarized excitation of the SL and GaAs barriers, obtained via the rate-equation analysis. The inset shows the typical rate-equation fitting results for the normalized sum of the σ^+- and σ^--polarized PL intensities at +1.0 and −1.0 V, under the excitation of the SL barrier.

analysis to determine the spin-injection time. Details regarding the rate equation are presented in the supplementary material. Here, rate-equation fitting was performed on the sum of the σ^+- and σ^--polarized PL intensities [see the inset in Fig. 3(c)]. The bias-voltage dependences of the spin-injection time under excitation of the SL and GaAs barriers are presented in Fig. 3(c). For the excitation of the GaAs barrier, the spin-injection time was almost independent of the bias voltage, with a value of ∼10 ps. However, for the excitation of the SL barrier, the spin-injection time increased significantly, from 10 ps at −1.0 V to 26 ps at +1.0 V. Here, note that even though the excitation energy changes from 1.51 eV (GaAs excitation) to 1.55 eV (SL excitation), the GaAs barrier just below the QDs is excited. As a result, the spin injection times at different excitation energies are similar under the negative bias voltages. As the InGaAs QDs are capped with heavily p-doped GaAs layer, the QDs are likely occupied with holes. Therefore, the PL rise time is determined by the electron transport time, i.e., the optically excited electrons at the SL barrier take longer time to arrive at the QDs compared to the electrons excited at the GaAs barrier. The multi-tunneling transport in the SL barrier is expected to be slower than the drift transport in the GaAs barrier. Although quantum tunneling of a single electron is typically very fast, the tunneling transport of collective electrons is discussed in this study. Electrons generated in the GaAs QWs close to the QDs can be injected, while electrons generated in the GaAs QWs far from the QDs can also be injected. Such a probabilistic behavior of collective electrons is expressed by the time constant of spin injection. Therefore, the far slower spin injection at +1.0 V indicated a dominant electron spin injection from the SL barrier into the QDs.

Figures 3(a) and 3(b) also show higher CPD values in the initial time region at +1.0 V than at −1.0 V (see the dashed green lines). The bias-voltage dependences of the initial CPD of the QD ES2 under the excitation of the SL and GaAs barriers are presented in Fig. 4(a). Here, the initial CPD is defined as the mean value near the CPD peak in the initial time region. As in the case of the bias-voltage dependence of the CPD shown in Fig. 2(d), the initial CPD was almost independent of the bias voltage under the excitation of the GaAs barrier,

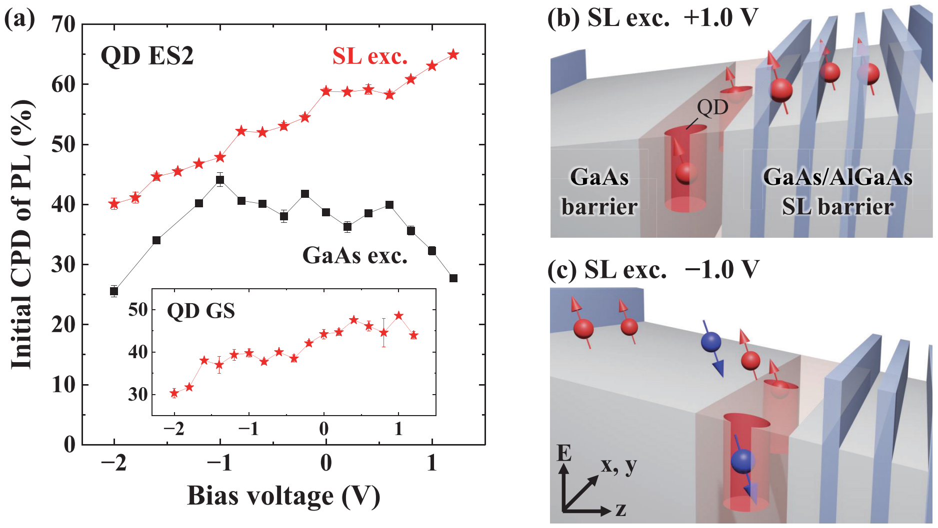

FIG. 4. (a) Bias-voltage dependence of the initial CPD of PL from QD ES2 under σ^+-polarized excitation of the SL and GaAs barriers, obtained via time-resolved analysis of the CPD. The inset shows the corresponding result for the QD GS under σ^+-polarized excitation of the SL barrier. Schematic of the electron spin injection dynamics in GaAs/Al$_{0.15}$Ga$_{0.85}$As SL and GaAs barriers under σ^+-polarized excitation of the SL barrier at (b) +1.0 and (c) −1.0 V.

whereas for the excitation of the SL barrier, it increased significantly, from 48% at -1.0 to 63% at $+1.0$ V. This trend was also observed in the QD GS (see the inset). The initial CPD of the QD ES2 was higher than the photogenerated electron spin polarization of 50%. This is attributed to the spin-dependent Pauli blocking of energy relaxation from the QD ES2 to the QD GS or QD ES1.[30] These results clearly indicate that the bias-voltage-dependent CPD properties of the QDs are mainly affected by the spin polarization of the injected electrons. Finally, we discuss the electric-field dependence of the electron spin injection dynamics under the excitation of the SL barrier. At $+1.0$ V, spin-polarized electrons were efficiently injected from the SL barrier into the QDs while maintaining a high degree of spin polarization via phonon-assisted tunneling [Fig. 4(b)], which resulted in the high CPD of the QD PL. In contrast, at -1.0 V, electron spin injection from the GaAs barrier into the QDs was dominant. In this case, the spin polarization of the injected electrons was reduced owing to the enhanced spin relaxation in the bulk GaAs barrier [Fig. 4(c)], resulting in the lower CPD of the QD PL. Therefore, we demonstrated that the optical spin polarization of QDs can be modulated via electric-field switching of the spin-injection layers. This method requires no precise control of the band potential, and thus, it can extend the studies on band engineering using external electric fields. The device performance can be improved by changing the combination of spin-injection layers, as well as the material used and its layer thickness.

In summary, we developed a QD-based electric-field-effect optical spin device with two different spin-injection layers, which consisted of a GaAs and GaAs/Al$_{0.15}$Ga$_{0.85}$As SL barriers. By switching the spin-injection layers using an external electric field, the spin polarization degree of electrons injected into the QDs can be changed for modulating the optical spin polarization of QDs. This was achieved by utilizing the difference in spin relaxation properties between the bulk GaAs and SL. Achieving significant modulation of the CPD by changing the combination of spin-injection layers can promote the development of circular-polarization modulation devices operating at ultrahigh speeds.

See the supplementary material for the sample growth conditions, structural characterization of the QDs, optical characterization methods, peak-fitting analysis of the PL spectra, and rate-equation analysis.

This work was financially supported by JSPS KAKENHI (Grants Nos. JP16H06359, JP20K20433, JP19K15380, JP21H01356, and JP21KK0068), JST FOREST (Grant No. JPMJFR202E), Advanced Technology Institute Research Grant 2021, Murata Science Foundation. Part of this work was conducted at Hokkaido University, with support from the "Nanotechnology Platform Program" of the Ministry of Education, Culture, Sports, Science and Technology (MEXT), Japan (Grant No. JPMXP09F20HK0010).

AUTHOR DECLARATIONS

Conflict of Interest

The authors have no conflicts to disclose.

Author Contributions

Hiroto Kise: Conceptualization (equal); Data curation (lead); Formal analysis (lead); Investigation (lead); Methodology (equal); Visualization (equal); Writing – original draft (lead). **Satoshi Hiura:** Conceptualization (lead); Data curation (equal); Formal analysis (equal); Funding acquisition (equal); Investigation (supporting); Methodology (equal); Project administration (lead); Supervision (lead); Writing – review & editing (lead). **Soyoung Park:** Formal analysis (supporting); Investigation (supporting); Writing – review & editing (supporting). **Junichi Takayama:** Formal analysis (supporting); Investigation (supporting); Software (equal); Writing – review & editing (supporting). **Kazuhisa Sueoka:** Writing – review & editing (supporting). **Akihiro Murayama:** Conceptualization (equal); Funding acquisition (lead); Methodology (equal); Project administration (equal); Supervision (equal); Writing – review & editing (equal).

DATA AVAILABILITY

The data that support the findings of this study are available from the corresponding author upon reasonable request.

REFERENCES

[1] M. Oestreich, J. Hübner, D. Hägele, P. J. Klar, W. Heimbrodt, W. W. Rühle, D. E. Ashenford, and B. Lunn, Appl. Phys. Lett. **74**, 1251 (1999).

[2] S. A. Wolf, D. D. Awschalom, R. A. Buhrman, J. M. Daughton, S. von Molnár, M. L. Roukes, A. Y. Chtchelkanova, and D. M. Treger, Science **294**, 1488 (2001).

[3] I. Žutić, J. Fabian, and S. Das Sarma, Rev. Mod. Phys. **76**, 323 (2004).

[4] D. D. Awschalom and M. E. Flatté, Nat. Phys. **3**, 153 (2007).

[5] Y. Ando, K. Hamaya, K. Kasahara, Y. Kishi, K. Ueda, K. Sawano, T. Sadoh, and M. Miyao, Appl. Phys. Lett. **94**, 182105 (2009).

[6] J. T. Heron, M. Trassin, K. Ashraf, M. Gajek, Q. He, S. Y. Yang, D. E. Nikonov, Y. H. Chu, S. Salahuddin, and R. Ramesh, Phys. Rev. Lett. **107**, 217202 (2011).

[7] R. Fiederling, M. Keim, G. Reuscher, W. Ossau, G. Schmidt, A. Waag, and L. W. Molenkamp, Nature **402**, 787 (1999).

[8] V. G. Truong, P. H. Binh, P. Renucci, M. Tran, Y. Lu, H. Jaffrès, J. M. George, C. Deranlot, A. Lemàtre, T. Amand, and X. Marie, Appl. Phys. Lett. **94**, 141109 (2009).

[9] M. Lindemann, G. Xu, T. Pusch, R. Michalzik, M. R. Hofmann, I. Žutić, and N. C. Gerhardt, Nature **568**, 212 (2019).

[10] A. E. Giba, X. Gao, M. Stoffel, X. Devaux, B. Xu, X. Marie, P. Renucci, H. Jaffrès, J.-M. George, G. Cong, Z. Wang, H. Rinnert, and Y. Lu, Phys. Rev. Appl. **14**, 034017 (2020).

[11] F. Cadiz, D. Lagarde, B. Tao, J. Frougier, B. Xu, X. Devaux, S. Migot, Z. G. Wang, X. F. Han, J. M. George, H. Carrere, A. Balocchi, T. Amand, X. Marie, B. Urbaszek, H. Jaffrès, Y. Lu, and P. Renucci, Phys. Rev. Mater. **4**, 124603 (2020).

[12] K. Etou, S. Hiura, S. Park, K. Sakamoto, J. Takayama, A. Subagyo, K. Sueoka, and A. Murayama, Phys. Rev. Appl. **16**, 014034 (2021).

[13] K. Etou, S. Hiura, S. Park, J. Takayama, A. Subagyo, K. Sueoka, and A. Murayama, Phys. Rev. Appl. **19**, 024055 (2023).

[14] F. Meier and B. Zakharchenya, *Optical Orientation* (Elsevier, North Holland, Amsterdam, 1984).

[15] H. J. Zhu, M. Ramsteiner, H. Kostial, M. Wassermeier, H. P. Schönherr, and K. H. Ploog, Phys. Rev. Lett. **87**, 016601 (2001).

[16] J. Heinrich, A. Huggenberger, T. Heindel, S. Reitzenstein, S. Höfling, L. Worschech, and A. Forchel, Appl. Phys. Lett. **96**, 211117 (2010).

[17] J. Beyer, I. A. Buyanova, S. Suraprapapich, C. W. Tu, and W. M. Chen, Appl. Phys. Lett. **98**, 203110 (2011).

[18] H. Chen, S. Hiura, J. Takayama, S. Park, K. Sueoka, and A. Murayama, Appl. Phys. Lett. **114**, 133101 (2019).

[19] M. Kroutvar, Y. Ducommun, D. Heiss, M. Bichler, D. Schuh, G. Abstreiter, and J. J. Finley, Nature **432**, 81 (2004).

[20] Y. Yang, Y. Zheng, W. Cao, A. Titov, J. Hyvonen, J. R. Manders, J. Xue, P. H. Holloway, and L. Qian, Nat. Photonics **9**, 259 (2015).

[21] S. Park, H. Chen, S. Hiura, J. Takayama, K. Sueoka, and A. Murayama, ACS Omega **6**, 8561 (2021).

[22] S. Park, S. Hiura, J. Takayama, K. Sueoka, and A. Murayama, Adv. Electron. Mater. **8**, 2200588 (2022).

[23] H. Sanada, I. Arata, Y. Ohno, Z. Chen, K. Kayanuma, Y. Oka, F. Matsukura, and H. Ohno, Appl. Phys. Lett. **81**, 2788 (2002).

[24] Y. Sato, Y. Takahashi, Y. Kawamura, and H. Kawaguchi, Jpn. J. Appl. Phys. **43**, L230 (2004).

[25] S. Hiura, K. Itabashi, K. Takeishi, J. Takayama, T. Kiba, and A. Murayama, Appl. Phys. Lett. **114**, 072406 (2019).

[26] S. Hiura, S. Hatakeyama, J. Takayama, and A. Murayama, Appl. Phys. Lett. **116**, 262407 (2020).

[27] S. Birner, T. Zibold, T. Andlauer, T. Kubis, M. Sabathil, A. Trellakis, and P. Vogl, IEEE Trans. Electron Devices **54**, 2137 (2007).

[28] T. Kiba, X. Yang, T. Yamamura, Y. Kuno, A. Subagyo, K. Sueoka, and A. Murayama, Appl. Phys. Lett. **103**, 082405 (2013).

[29] T. Yamamura, T. Kiba, X. Yang, J. Takayama, A. Subagyo, K. Sueoka, and A. Murayama, J. Appl. Phys. **116**, 094309 (2014).

[30] V. K. Kalevich, M. Paillard, K. V. Kavokin, X. Marie, A. R. Kovsh, T. Amand, A. E. Zhukov, Y. G. Musikhin, V. M. Ustinov, E. Vanelle, and B. P. Zakharchenya, Phys. Rev. B **64**, 045309 (2001).